Tabata, *Polym. Prepr., Am. Chem. Soc., Div. Polym. Chem.*, **20**, 372 (1979).
(28) S. Egusa, K. Ishigure, and Y. Tabata, *Macromolecules*, submitted.
(29) S. An, T. Tamura, A. Furuhashi, and H. Wakabayashi, *Proc. Int. Symp. Phys. Fast Reactors*, **1**, 152 (1973).
(30) S. Egusa, K. Ishigure, S. Tagawa, Y. Tabata, and K. Oshima, *Radiat. Phys. Chem.*, **11**, 129 (1978).
(31) J. Cazes and R. J. Dobbins, *J. Polym. Sci., Polym. Lett. Ed.*, **8**, 785 (1970).
(32) E. Cohn-Ginsberg, T. G. Fox, and H. F. Mason, *Polymer*, **3**, 97 (1962).
(33) C. J. Hochanadel, "Comparative Effects of Radiation", M. Burton, et al., Eds., Wiley, New York, 1960, p 174.
(34) G. Beck, D. Lindenau, and W. Schnabel, *Macromolecules*, **10**, 135 (1977).
(35) H. Yamakawa, M. Sakaguchi, and J. Sohma, *Rep. Prog. Polym. Phys. Jpn.*, **19**, 477 (1976).
(36) M. Tabata, K. Takahashi, H. Yamakawa, and J. Sohma, *Rep. Prog. Polym. Phys. Jpn.*, **20**, 531 (1977).
(37) A. Todd, *J. Polym. Sci.*, **42**, 223 (1960).
(38) C. David, D. Fuld, and G. Geuskens, *Makromol. Chem.*, **139**, 269 (1970).
(39) H. Hiraoka, *IBM J. Res. Dev.*, **21**, 121 (1977).

Dimensional Changes Accompanying the Formation of Poly(oxyethylene) Macrocycles

Wayne L. Mattice

Department of Chemistry, Louisiana State University, Baton Rouge, Louisiana 70803.

Received February 12, 1979

ABSTRACT: Cyclization of poly(oxyethylene) to form the macrocycle $3x$-crown-x, i.e., $(\text{-CH}_2\text{CH}_2\text{O-})_x$, has been studied for even x from 4 to 20 using Monte-Carlo methods. Poly(oxyethylene) is assumed to behave in accord with the model developed by Mark and Flory. The fraction of acyclic chains satisfying criteria for cyclization reached a maximum of 1.2×10^{-3} for $x = 6$ and fell off to 0.1×10^{-3} when x was 20. The implication that 18-crown-6 is the most easily formed macrocycle is in harmony with experiment. Cyclization to form the larger macrocycles requires a reduction of $\langle L_1^2 \rangle$ by a factor of approximately 2, along with comparatively minor changes in $\langle L_2^2 \rangle$ and $\langle L_3^2 \rangle$. Here $L_1^2 \geq L_2^2 \geq L_3^2$ are the principal moments of the inertia tensor for the oxygen atoms, and angle brackets denote the average over all conformations. Cyclization to form crowns of the size investigated causes a reduction in the fraction of C–C bonds adopting trans placements. However, there is no significant change in the population of trans states at C–O bonds. The macrocycles 18-crown-6 and 24-crown-8 have definite preferences for certain spatial distributions of their oxygen atoms. Larger macrocycles are more flexible and show no great preference for a particular conformation. Among the most favored conformations for 18-crown-6 is the one seen in its complex with potassium ion. In contrast, metal-free 18-crown-6 crystallizes in a conformation which is occupied by only about 1% of the macrocycles in the unperturbed state.

Cyclization of moderately long chain molecules is an area of considerable current interest.[1] For example, a large variety of synthetic and naturally occurring macrocycles exhibit interesting ion-binding properties.[2-4] Many of these synthetic macrocycles consist wholely or in part of poly(oxyethylene).[2,5] As the size of a poly(oxyethylene) macrocycle increases, ring flexibility will eventually make it no longer profitable to attempt an explanation of molecular properties in terms of a small number of conformations. One current objective is to define the macrocycle size where this effect occurs for cyclic poly(oxyethylene). Especially favored conformations for smaller macrocycles will also be characterized. Finally, average conformation-dependent properties for both small and large macrocycles will be described, as well as changes in these properties accompanying cyclization. All calculations are based on a rotational isomeric state model[6-8] for unperturbed poly(oxyethylene) which is in harmony with measured unperturbed dimensions and dipole moments, as well as their temperature coefficients.

Calculational Method

Calculations are based on an adaptation of the macrocyclization theory utilized by Flory and co-workers.[9] It is conveniently described with the aid of Figure 1, which schematically depicts an acyclic $\text{CH}_3\text{O}(\text{CH}_2\text{CH}_2\text{O})_x\text{CH}_3$ in a conformation nearly compatible with cyclization. The bond vector from chain atom $i - 1$ to chain atom i is denoted $\mathbf{l}_i$. The initial CH_3–O bond is ignored in this numbering scheme, and the first oxygen atom is designated chain atom zero. The vector $\mathbf{r}$ is drawn from oxygen atom 0 to oxygen atom $3x$. Its length is zero in the cyclic molecule containing x oxygen atoms. (Such cyclic molecules are frequently denoted $3x$-crown-x.) Successful cyclization also requires the angle between $\mathbf{l}_1$ and $\mathbf{l}_{3x}$ be sufficiently close to the normal ∠C–O–C of 110°.

Representative chains were generated using the rotational isomeric state treatment developed by Mark and Flory[6,7] for poly(oxyethylene). Their treatment successfully accounts for experimentally observed unperturbed dimensions and dipole moments, as well as their temperature dependence. It has recently been used to account for an unusual temperature dependence in the NMR spectrum of certain poly(oxyethylene)macrocycles containing a 2,2′-bipyridyl subunit.[10] Chain geometry has bond lengths of 1.43 Å (C–O) and 1.53 Å (C–C), and bond angles are 110°. Three rotational states (trans, gauche±) are available to each internal bond. Their dihedral angles are 0 and ±120°. Conditional and a priori probabilities were evaluated at 25 °C using the interaction energies assigned by Mark and Flory[6,7] and the appropriate rotational isomeric state formalism.[11] Conditional probabilities, in their matrix representation, are

$$\text{C–C bond} \quad \begin{bmatrix} 0.2050 & 0.3975 & 0.3975 \\ 0.2491 & 0.4832 & 0.2676 \\ 0.2491 & 0.2676 & 0.4832 \end{bmatrix} \tag{1}$$

$$\text{C–O bond} \quad \begin{bmatrix} 0.7247 & 0.1376 & 0.1376 \\ 0.7721 & 0.1466 & 0.0812 \\ 0.7721 & 0.0812 & 0.1466 \end{bmatrix} \tag{2}$$

$$\text{O–C bond} \quad \begin{bmatrix} 0.7352 & 0.1324 & 0.1324 \\ 0.8474 & 0.1526 & 0 \\ 0.8474 & 0 & 0.1526 \end{bmatrix} \tag{3}$$

Columns index the state of the bond in question, while

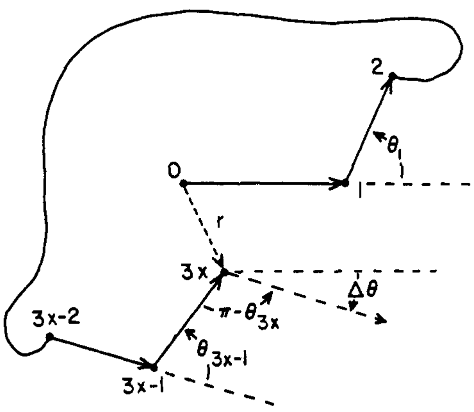

Figure 1. Schematic acyclic poly(oxyethylene) chain in a conformation nearly consistent with cyclization.

rows index the state of the preceeding bond. The order of indexing is trans, gauche$^+$, gauche$^-$. A priori probabilities for the first O–C bond were 0.2155, 0.3923, and 0.3923. Representative chains were generated using these probabilities in conjunction with a random-number generator.

Average Properties of Acyclic and Cyclic Molecules

Acyclic Chains. Average properties for acyclic $CH_3O(CH_2CH_2O)_xCH_3$ ($x > 1$) were deduced from a sample of at least 4000 $(x + 2)$ chains. The chain with $x = 1$ was treated by direct enumeration of all conformations. Of major interest in the present paper is the spatial distribution of the oxygen atoms. It was evaluated by first computing the moment of inertia tensor, $\mathbf{S}_{x2}$, for the oxygen atoms in each chain generated.

$$\mathbf{S}_{x2} = n^{-1}\sum \mathbf{r}^{x2} - \mathbf{g}^{x2} \tag{4}$$

$$\mathbf{g} = n^{-1}\sum \mathbf{r} \tag{5}$$

Here $\mathbf{r}$ is the vector from the first oxygen atom to the nucleus of another oxygen atom, summations extend over all n oxygen atoms, and the superscript $x2$ denotes the self-direct product. Note that $n = x + 1$ for acyclic molecules, while $n = x$ for macrocycles formed from the acyclic chains. This procedure generates $\mathbf{S}_{x2}$ as a column comprised of the nine elements arranged in reading order.[12] Conversion to the 3 × 3 form, followed by diagonalization, yields the principal moments, $L_1^2 \geq L_2^2 \geq L_3^2$. Corresponding moments for all chains in a sample were averaged to yield $\langle L_1^2\rangle$, $\langle L_2^2\rangle$, and $\langle L_3^2\rangle$. The mean-square unperturbed radius of gyration, $\langle s^2\rangle_0$, is their sum.

A convenient representation for $\langle s^2\rangle_0$ is as the characteristic ratio, defined as $\langle s^2\rangle_0/n$ (6.43 Å^2). The sum of the squared lengths of two C–O and one C–C bond is 6.43 Å. Results are depicted in Figure 2. The characteristic ratio attains a limiting value of 0.65 as $n \rightarrow \infty$, in accord with experimentally determined values.[6,13,14] This result also is in harmony with that obtained by matrix methods which achieve an exact averaging over all conformations.[6]

Asymmetry of individual conformations is assessed through examination of $\langle L_i^2\rangle/\langle L_1^2\rangle$, $i = 2, 3$. These ratios are also depicted in Figure 2. They increase with n, attaining limiting values of 0.23 for $i = 2$ and 0.076 for $i = 3$. Equivalent treatment of unperturbed poly(methylene) chains yields limiting values of about $^1/_3$ and $^1/_{12}$.[15] Individual chains tend to have a higher assymmetry for poly(oxyethylene) than for poly(methylene).

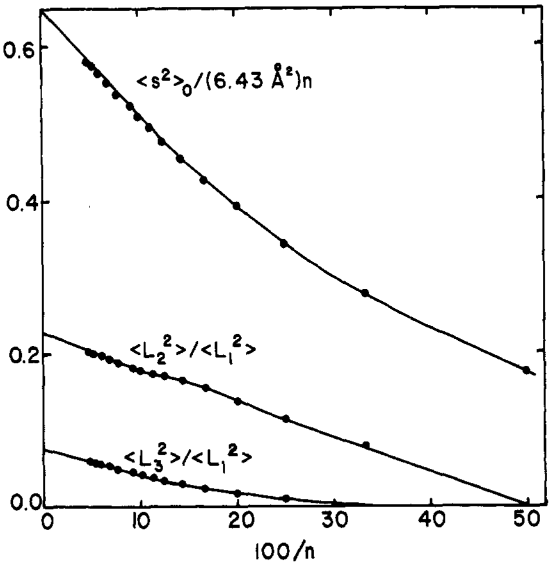

Figure 2. Mean-square radius of gyration and $\langle L_i^2\rangle/\langle L_1^2\rangle$, $i = 2, 3$, for unperturbed acyclic poly(oxyethylene) chains containing n oxygen atoms.

Table I
Chains Meeting Criteria for Cyclization

x	no. of chains generated (thousands)	no. of cyclic chains	fraction cyclic ($\times 10^5$)
4	24	1	4
6	32	38	119
8	80	23	29
10	120	14	12
12	140	16	11
14	150	12	8
16	150	15	10
18	150	13	9
20	165	15	9

Ease of Cyclization. Chains generated in the samples described above for even x ($x \geq 4$) were examined for fulfillment of criteria for successful cyclization. The cyclic molecule contains x oxygen atoms (terminal methyl groups are ignored) and may be denoted $3x$-crown-x. Terminal oxygen atoms must therefore occupy the same position in a particular chain if cyclization is successful. This requirement was assumed to be satisfied for molecules with $x \leq 10$ if the nuclei were separated by no more than 0.55 Å. A second requirement for successful cyclization is that the angle between the first $O–CH_2$ bond and the last $CH_2–O$ bond be sufficiently close to the expected value (110°). This requirement was assumed to be satisfied for these molecules if the actual value was 110 ± 3°.

The above tolerances were chosen on the basis of preliminary calculations executed for formation of 18-crown-6. Calculations using a small tolerance for $\Delta\theta$ yielded a few conformations with $\Delta r < 0.55$ Å, a multitude with $\Delta r > 4.4$ Å, but none with 0.55 Å $< \Delta r <$ 4.4 Å. Similarly, calculations using a small tolerance for Δr yielded a few conformations with $\Delta\theta < 2°$, many with $\Delta\theta > 12°$, but none with $2° < \Delta\theta < 12°$. This behavior arises because the chain is nearly constrained to follow a diamond lattice. A slight departure from the diamond lattice occurs because bonds are not precisely of the same length and bond angles are not precisely tetrahedral. Tolerances for cyclization were relaxed to $\Delta r \leq 0.8$ Å and $\Delta\theta \leq 5°$ for $x \geq 12$.

Table I presents the number of chains generated at each x and the number satisfying criteria for successful cyclization. Cyclization is most readily achieved when x is six. It is of interest to ascertain whether this result is in harmony with actual experimental work. An unequivocal

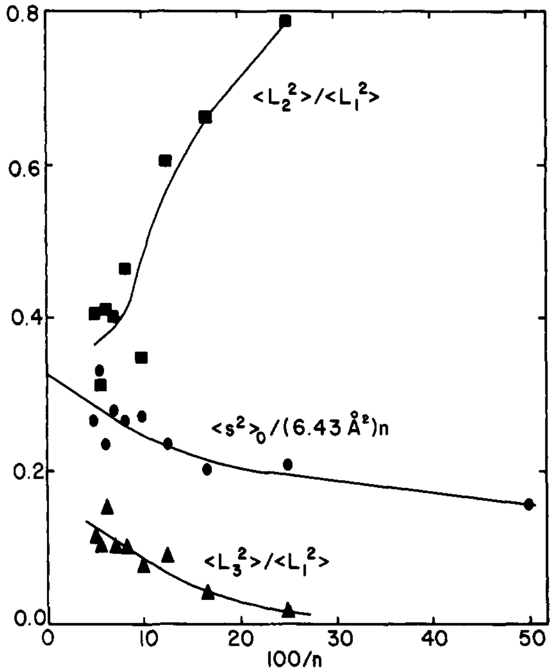

Figure 3. Mean-square radius of gyration and $\langle L_i^2\rangle/\langle L_1^2\rangle$, i = 2, 3, for poly(oxyethylene)macrocycles (3*n*-crown-*n*) whose occurrence is summarized in Table I.

comparison is not possible because a metal is used as a template ion in experimental cyclizations. Nevertheless, there is evidence that cyclization is most readily effected when x is 6. Yields for formation of 12-crown-4, 18-crown-6, and 24-crown-8 are 13, 30–93, and 15%, respectively.[16,17]

A previous Monte-Carlo study[18] of the cyclization of poly(oxyethylene) reaches conclusions not entirely compatible with those derived from Table I. Specifically, the earlier study found the probability for cyclization was maximal at x = 4 or 5, decreased with increasing x, and virtually vanished at x = 20. Different conclusions arise in part from the criteria used for successful cyclization. In the earlier study, cyclization was achieved if the end-to-end distance did not exceed 4 Å. No restriction whatsoever was imposed on the value of the bond angle formed upon ring closure. The earlier work also specifically rejected chain conformations containing skeletal overlaps. Assembly of our successful cyclic chains, using CPK molecular models, reveals the conclusions would not be modified if we rejected conformations with skeletal overlaps. Our use of $\angle$C–O–C = 110° ± $\Delta\theta$ for ring closure may have been helpful in elimination of self-interacting chains. The two studies also contain minor differences in the statistical weights and dihedral angles used for the gauche states.

Alteration in $\langle s^2\rangle_0$ and $\langle L_i^2\rangle$ upon Cyclization. Figure 3 depicts the average dimensions of cyclic chains containing an even number of oxygen atoms. The chair conformation of 1,4-dioxane is used for 6-crown-2. Properties of the remaining crowns were evaluated from the surviving chains whose occurrence is summarized in Table I. The scatter is much greater in Figure 3 than in Figure 2, due to the much smaller sample size for cyclic molecules. Despite the scatter, certain trends are readily apparent.

As expected, cyclization reduces $\langle s^2\rangle_0$. Application of random-flight statistics leads to the prediction that $\langle s^2\rangle_0$ for a large cyclic molecule should be half that for the corresponding acyclic chain.[19] The intercept at $1/n$ = 0 in Figure 3 is based on this prediction. It clearly represents a reasonable extrapolation of the data. Results for most of the macrocycles are in surprisingly good agreement with the random-flight prediction. For those chains with n = 6, 8, ..., 20, the ratio $\langle s^2\rangle_{0,\mathrm{cyclic}}/\langle s^2\rangle_{0,\mathrm{acyclic}}$ lies in the range 0.42–0.58, and its average is 0.50.

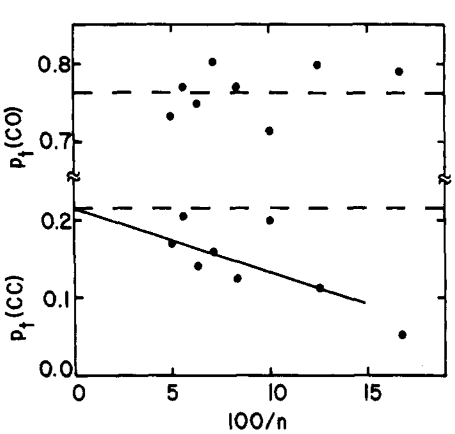

Figure 4. A priori probability of trans placements at C–O and C–C bonds in the poly(oxyethylene) macrocycles (3*n*-crown-*n*) whose occurrence is summarized in Table I. Horizontal dashed lines are drawn at the values found for long unperturbed acyclic chains.

Cyclization not only alters $\langle s^2\rangle_0$ but also has pronounced effects on the asymmetry of the spatial distribution. A comparison of $\langle L_2^2\rangle/\langle L_1^2\rangle$ in Figures 2 and 3 reveals a dramatic increase upon cyclization for the smaller chains. An increase by about a factor of 2 persists for even the largest macrocycle studied (60-crown-20). Scatter in the data, however, prohibits an unambiguous statement concerning much larger macrocycles. While it may be tempting to extrapolate $\langle L_2^2\rangle/\langle L_1^2\rangle$ in Figure 3 to an intercept near 1/3, an appreciably lower intercept cannot be excluded. The other ratio of interest, $\langle L_3^2\rangle/\langle L_1^2\rangle$, also increases upon cyclization. While extrapolation to $1/n$ = 0 in Figure 3 is not uniquely defined, it is apparent that any reasonable extrapolation will yield an intercept larger than that obtained in Figure 2 for the acyclic molecules.

Changes in the $\langle L_i^2\rangle$ upon cyclization for the larger chains studied (n = 10, 12, ..., 20) are also of interest. The factors by which the averaged moments are reduced are 0.42 (0.06), 0.84 (0.10), and 0.87 (0.07) for i = 1–3, respectively. (Standard deviations are in parentheses.) Cyclization of chains of this size demands a major contraction along the largest principal axis. Contraction along the remaining principal axes is comparatively minor.

Further insight into the conformational consequences of cyclization is achieved by examination of the occurrence of trans and gauche placements at the C–C and C–O bonds. Long acyclic poly(oxyethylene) chains have trans placements at 76% of their C–O bonds and 21.5% of their C–C bonds. These values are denoted by the horizontal dashed lines in Figure 4. Points in this figure denote the fraction of the appropriate bond having trans placements in the crowns. Cyclization for those chains with $n \geq 6$ is achieved with almost no alteration in the a priori probability of a trans placement at C–O bonds. Trans placements at C–C bonds, on the other hand, become less likely upon cyclization of chains of small to moderate size. This effect decreases in importance as the size of the macrocycle increases.

Macrocycle Conformations Seen with Exceptional Frequency

Table I demonstrates that several cyclic chains were identified at each n for $n \geq 6$. We now inquire whether specific conformations of these macrocycles are seen with

Table II
Macrocycle Oxygen-Atom Distributions Encountered More Than Once

	n^a	N^b	N'^c	s^2, Å^2	L_1^2, Å^2	L_2^2, Å^2	L_3^2, Å^2	p_i^d
A	6	9	2	8.0	4.0	4.0	0.0	0.41
B	6	9	4	8.0	5.1	2.9	0.0	0.14
C	6	7	4	7.4	4.0	3.1	0.3	0.25
D	6	5	5	7.3	4.2	2.8	0.4	0.18
E	6	2	1	9.4	7.0	2.4	0.0	0.01
F	8	8	2	13.0	6.3	6.3	0.4	0.74
G	8	2	2	10.2	5.6	3.6	1.0	0.03

[a] Number of oxygen atoms in the macrocycle. [b] Number of cyclic chains with the indicated $\mathbf{S}_{x_2}$, evaluated for oxygen atoms only. [c] Number of different $\mathbf{S}_{x_2}$ for the N chains *if* both carbon and oxygen atoms were included in evaluation of the moment of inertia tensor. [d] Fraction of 3n-crown-n molecules having the indicated oxygen atom distribution, based on an approximation to the configuration partition function for these molecules (see text).

special frequency. Attention will be focused on the spatial distributions of their oxygen atoms, as reflected by the L_i^2. The objective is to identify and characterize all cases where two or more of the crowns generated have identical $\mathbf{S}_{x2}$ (evaluated for the oxygen atoms only). Results are summarized in Table II. One of the most striking features is the absence of any entry for $n \geq 10$. Even though 12–16 cyclic chains were identified at these n, no two had the same distribution of oxygen atoms. No single conformation dominates the distribution for macrocycles of this size. In contrast, 18-crown-6 and 24-crown-8 have definite preferences for certain spatial distributions of their oxygen atoms.

18-Crown-6. The entry denoted **A** in Table II has $L_1^2 = L_2^2$, $L_3^2 = 0$. Its oxygen atoms describe a regular hexagon. Seven of the nine cyclic chains have the conformation $(-tg^{\pm}t-tg^{\mp}t-)_3$, where all C–O bonds occupy trans placements while all C–C bonds have gauche placements. A cavity is present, with oxygen atoms lining the cavity. The relative weights for the 18-crown-6 conformations generated might vary somewhat from that deduced from the size of N in Table II. This problem arises because only a small fraction of the large number of chains generated satisfies the stringent requirements for cyclization. An alternative assessment of the relative weights is obtained from

$$p_i = Z_{\text{cyc}}^{-1} g_i \exp(-E_i/RT) \quad (6)$$

$$Z_{\text{cyc}} = \sum g_i \exp(-E_i/RT) \quad (7)$$

where Z_{cyc} is an approximation to the configuration partition function for the crown. It is a sum of the product of a degeneracy and Boltzmann factor. The sum extends only over the *distinct* cyclic chain conformations *actually generated.* Thus p_i will correctly evaluate the *relative* weights of these conformations. It will, however, overestimate the fraction of chains with a given conformation if certain possible cyclic chains were not generated in the Monte-Carlo sample and therefore make no contribution to Z_{cyc} in eq 7. The p_i evaluated in this manner are presented in the final column in Table II. The most likely oxygen atom distribution is that denoted by **A**. The single distinct chain conformation $(-tg^{\pm}t-tg^{\ddagger}t-)_3$ itself merits a p_i of 0.38.

The second entry in Table II has the same s^2 as **A**, but it differs in the asymmetry of $\mathbf{S}_{x^2}$. This entry still has $L_3^2 = 0$, but now $L_1^2 > L_2^2$. Oxygen atoms in **C** and **D** lie significantly out of the best plane through these atoms ($L_3^2 > 0$). An oxygen-lined cavity is present in **B**, **C**, and **D**, but it is partially blocked by a methylene or ethylene group in some chain conformations. The most prevalent chain conformations in **B**, **C**, and **D** are $(-tg^{\pm}t-tg^{\pm}t-g^{\pm}g^{\pm}t-tg^{\mp}t-tg^{\mp}t-g^{\mp}g^{\mp}t-)$, $(tg^{\pm}t-tg^{\mp}t-tg^{\pm}g^{\pm}-tg^{\pm}t-tg^{\mp}t-g^{\mp}g^{\mp}t-)$, and $(-tg^{\pm}t-tg^{\mp}t-tg^{\pm}t-tg^{\pm}g^{\mp}-tg^{\pm}t-g^{\mp}g^{\mp}t-)$, respectively.

Gauche placements were found about *all* of the C–C bonds in the 18-crown-6 molecules having oxygen atom tensors **A**, **B**, **C**, and **D**. In contrast, the chain conformation for **E** $(-ttt-tg^{\pm}t-tg^{\mp}g^{\pm}-ttt-tg^{\mp}t-tg^{\pm}g^{\mp}-)$ has trans placements at two of the six C–C bonds. These trans placements produce an elongation of the crown, as is evident from the increase in L_1^2. Only two of the six oxygen atoms line the narrow cavity. Two methylene groups, one from each *–ttt–* segment, intrude into this cavity.

Special interest attends **E** because it is the conformation assigned to 18-crown-6 in the crystalline state, first on the basis of infrared spectroscopy[20] and subsequently by X-ray diffraction studies.[21] A stereoscopic view has been presented by Dunitz et al.[21] While rather sharp infrared bands are obtained from crystalline 18-crown-6, bands obtained from the liquid are very broad.[20] Broadening has been attributed to either an increase in vibrational amplitude or admixture of additional conformers.[20] The present work provides support for the latter explanation. Only about 5% of the 18-crown-6 molecules generated have oxygen tensor **E**, and the p_i suggests an even lower occurrence. We note that **E** has two runs of four successive trans placements, while **A**, **B**, **C**, and **D** never have more than two successive bonds occupying trans placements. The observed crystallization as **E** could be rationalized if the longer runs of trans placements permit more favorable intermolecular interactions in the solid state.

One measure of the size of the oxygen-lined cavity in 18-crown-6 is provided by the *smallest* separation of oxygen atoms connected by nine covalent bonds. By this criterion, cavity size increases as **E** < **B** = **C** = **D** < **A**, dimensions beings 3.9, 4.6, and 5.7 Å. The **A** conformation is unique because of its high symmetry. Roughly 40% of unperturbed 18-crown-6 has this oxygen atom tensor, as estimated from p_i. A recent study[22] found cation binding to 18-crown-6 increased as Na^+ (4.7 Å) = Cs^+ (6.1 Å) < Ag^+ (5.3 Å) = Rb^+ (5.8 Å) < K^+ (5.5 Å) < Tl^+ (5.6 Å). Figures in parentheses are the sum of the van der Waals diameter of an ethereal oxygen atom and the ionic diameter of the cation. This sum for the strongly binding ions is close to the size of the oxygen-lined cavity in **A**. Potassium, rubidium, and cesium ions form a complex with the $(-tg^{\pm}t-tg^{\mp}t-)_3$ conformation of 18-crown-6 in the solid state.[20,21] The oxygen atom tensor differs slightly from that of **A** because gauche states have dihedral angles of ±115° rather than ±120°.[21] A different conformation occurs in the complex of sodium ion with 18-crown-6.[21]

24-Crown-8. The entry denoted **F** in Table II has $L_1^2 = L_2^2$. It is a slightly distorted octagon when viewed along the axis whose principal moment is L_3^2. Six of the eight **F** entries arise from the the chain conformation $(-tg^{\pm}t-$

$tg^{\pm}t{-}tg^{\mp}t{-}tg^{\mp}t{-})_2$, which yields a large oxygen-lined hole. Oxygen atoms connected by 12 covalent bonds are separated by 7.1 Å. Infrared spectroscopy demonstrates that 24-crown-8 adopts this conformation in the crystalline state.[20]

Acknowledgment. The author wishes to thank Professors George Newkome and Richard Gandour for their helpful comments on an early version of this paper. Supported by NSF Grant No. PCM 76-23235.

References and Notes

(1) J. A. Semlyen, *Adv. Polym. Sci.*, **21**, 41 (1976).
(2) J. J. Christensen, J. O. Hill, and R. M. Izatt, *Science*, **174**, 459 (1971).
(3) F. A. Bovey, A. I. Brewster, D. J. Patel, A. E. Tonelli, and D. A. Torchia, *Acc. Chem. Res.*, **6**, 193 (1972).
(4) C. M. Deber, V. Madison, and E. R. Blout, *Acc. Chem. Res.*, **9**, 106 (1976).
(5) C. J. Pedersen, *J. Am. Chem. Soc.*, **89**, 7017 (1967).
(6) J. E. Mark and P. J. Flory, *J. Am. Chem. Soc.*, **87**, 1415 (1965).
(7) J. E. Mark and P. J. Flory, *J. Am. Chem. Soc.*, **88**, 3702 (1966).
(8) A. Abe and J. E. Mark, *J. Am. Chem. Soc.*, **98**, 6468 (1976).
(9) P. J. Flory, U. W. Suter, and M. Mutter, *J. Am. Chem. Soc.*, **98**, 5733 (1976).
(10) W. L. Mattice and G. R. Newkome, *J. Am. Chem. Soc.*, in press.
(11) P. J. Flory, *Macromolecules*, **7**, 381 (1974).
(12) P. J. Flory and D. Y. Yoon, *J. Chem. Phys.*, **61**, 5358 (1974).
(13) F. E. Bailey, Jr., and R. W. Callard, *J. Appl. Polym. Sci.*, **1**, 56 (1959).
(14) F. E. Bailey, Jr., J. L. Kucera, and L. G. Inhof, *J. Polym. Sci.*, **32**, 517 (1958).
(15) D. Y. Yoon and P. J. Flory, *J. Chem. Phys.*, **61**, 5366 (1974).
(16) R. N. Greene, *Tetrahedron Lett.*, 1793 (1972).
(17) F. L. Cook, T. C. Caruso, M. P. Byrne, C. W. Bowers, D. H. Speck, and C. L. Liotta, *Tetrahedron Lett.*, 4029 (1974).
(18) M. Sisido, Y. Imanishi, and T. Higashimura, *Bull. Chem. Soc. Jpn.*, **51**, 1469 (1978).
(19) H. A. Kramers, *J. Chem. Phys.*, **14**, 415 (1946).
(20) J. Dale and P. O. Kristiansen, *Acta Chem. Scand.*, **26**, 1471 (1972).
(21) J. D. Dunitz, M. Dobler, P. Seiler, and R. P. Phizackerley, *Acta Crystallogr., Sect. B*, **30**, 2733 (1974).
(22) R. M. Izatt, R. E. Terry, B. L. Haymore, L. D. Hansen, N. K. Dalley, A. G. Avondet, and J. J. Christensen, *J. Am. Chem. Soc.*, **98**, 7620 (1976).

Vibrational Spectra of Polymers. 2.[1] Variable-Temperature Raman Spectroscopy as a Probe for Ion Clustering in Ionomers

Anton Neppel, Ian S. Butler,* and Adi Eisenberg

Department of Chemistry, McGill University, Montreal, Quebec, Canada H3A 2K6.

Received March 19, 1979

ABSTRACT: The Raman spectra of a series of ethyl acrylate–sodium acrylate copolymers with sodium acrylate contents varying from zero to 100 mol % have been measured in the 425–100-cm^{-1} region at room temperature, 150, 200, and 250 °C. The bands observed at 246 and 175 cm^{-1} have been attributed to ion multiplets and clusters, respectively. At all four temperatures investigated, the intensities of the multiplet and cluster bands increase steadily with increasing sodium acrylate content up to ca. 10 and 35 mol %, respectively, and thereafter remain essentially composition invariant. With increasing temperature, the multiplet band intensity increases while the cluster band intensity decreases throughout the complete composition range studied. A similar variable-temperature Raman study was also carried out for a series of styrene–sodium methacrylate ionomers, in which the band intensities showed practically no variation with temperature. The results of both studies indicate that the variation with temperature of the ion contents in multiplets and clusters is strongly dependent on the proximity to the glass-transition temperature. Furthermore, it is seen that the total amount of ions in clusters or multiplets depends on the dielectric constant of the polymer, a high dielectric constant favoring multiplets at the expense of clusters.

Recent studies on ion-containing polymers, such as the copolymers of ethylene, butadiene, or styrene with acrylic acid salts, have shown that the state of aggregation of the ions has considerable influence on the mechanical and rheological properties of these materials.[2-7] Most investigations have been focused on ionomers having ionic component concentrations below 10–15 mol %. In this composition range, the ionic sites of the polymer chains and the metal ions form ion pairs due to the low dielectric constant of the major component present (e.g., ethylene, butadiene, styrene, etc.). These ion pairs are thought to associate further into multiplets of a few ion pairs and into larger entities called clusters.[8] The latter are surrounded by the matrix which consists of the polymer chains and the multiplets.

Multiplet and cluster formation in ethyl acrylate–sodium acrylate copolymers was initially deduced from an accelerated rise of the glass-transition temperature (T_g) with increasing ion concentration.[9] This occurred at approximately the same sodium acrylate concentration at which time–temperature superposition in viscoelastic measurements failed (12–16 mol %),[10] since the latter phenomenon is also associated with clustering. Thus, it was concluded that the clusters dominate the rheological behavior above ca. 12 mol % of ions, whereas the multiplets are of primary importance below this concentration. No information, however, was available from these studies as to the relative numbers of ion pairs in multiplets or clusters at a given ion content.

Vibrational spectroscopy has rarely contributed to the elucidation of supermolecular structure.[3] Infrared results have been claimed to show ionic aggregation in ethylene- and butadiene-based copolymers of methacrylic acid salts.[11-14] Also, Rouse et al.[14] have attributed specific bands in the far-infrared spectra of styrene–metal methacrylate ionomers to multiplets and clusters. Recently, we have found a quantitative linear correlation between the intensities of the low-energy Raman bands associated with the multiplets and the clusters in the same ionomers and the multiplet and cluster concentrations obtained from